Synthesis of carbon nanotubes with chemical vapor deposition by using milled iron catalyst

ÖMER GÜLER*, ERTAN EVIN, S. HALE GÜLER
Department of Metallurgy and Materials Engineering, Fırat University, Elazığ 23119, Turkey

In this study, carbon nanotubes were synthesized by chemical vapor deposition (CVD) process. In CVD process, milled iron powders were used as catalyst. Initially, iron powders were milled by high energy ball mill for 3h. Then, iron particles were homogeny distributed onto substrate and carbon nanotubes were obtained by CVD process inside tube reactor. Carbon nanotubes were investigated by HR-TEM to determine the effect of milled iron catalyst on nanotube formation.

(Received April 18, 2012; accepted September 18, 2013)

Keywords: Carbon nanotubes, Chemical vapor deposition, catalyst

1. Introduction

Carbon nanotubes (CNTs) are crystalline graphitic sheets rolled up into a seamless cylindrical shape [1]. Since their discovery diverse and unique physical properties of CNTs have been revealed. They have attracted considerable interest by many scientists due to their extraordinary chemical, electronic, thermal, and mechanical properties. Their special properties make CNTs potential candidates for many application areas such as field emission devices [2], scanning probes, nanoscale electronic devices [3], hydrogen storage, chemical sensors, and composite reinforcing materials [4]. CNTs are known to have better properties in the axial direction than in the transverse direction. CNTs were synthesized by many methods such as; CVD, laser ablation, arc-discharge, sol-gel, PECVD. Even, some researchers were successfully obtained by mechano-thermal process (having short-time milling) [5]. But, CNTs are usually synthesized by laser ablation of carbon rods, direct current arc- discharge between electrodes [6], or chemical vapor deposition (CVD) [7,8]. Compared to arc discharge and laser ablation, CVD allows large amounts of high purity and aligned nanotubes to be obtained. The basic mechanism of the growth of CNTs involves dissociation of hydrocarbon molecules over metal clusters heated to high temperatures (700–900 ^{o}C). The metal clusters acting as a catalyst can be created by different techniques, for instance by vapour or sputter deposition of a thin metallic layer on the substrate, by impregnation of porous materials by metals, by deposition of solutions or suspensions of substances containing catalyzing metals or by admission of organometallic substances into the reaction chamber [8–12].

2. Experimental

For synthesis of carbon nanotubes, iron was used as catalyst. Iron powders (Merck 103800, particle size 150 μm) were milled by high energy ball milling for 3 h to decrease the particle size and to active. Carbon nanotubes were grown onto p-doped Si (1 0 0) substrates that were rinsed consecutively in acetone and ethanol in an ultrasonic bath prior to introduction in the vacuum chamber. No further in situ cleaning procedure was performed. Activated iron particles were homogeny distributed onto substrate. Substrate were placed in a quartz boat and then inserted into the centre of quartz tube reactor housed in a furnace. The tube was evacuated at a base pressure of 10^{-3} Torr by a vacuum pump for purged. Then the furnace was heated to 650 ^{o}C in atmosphere of Ar gas (1 l/min) at 2 Torr. At 650 ^{o}C, C_2H_2 gas flow at the same pressure for 40 min. Then, the cooling process of furnace occurred in Ar atmosphere. The structural changes of the milled iron powders were investigated by using Bruker X-ray diffractometer (XRD) with CuKα radiation. Samples were investigated via JEOL JEM 2100F model High-Resolution Transmission Electron Microscopy (HR-TEM). Chemical compositions were examined by using Oxford instrument Energy dispersive X-ray (EDX) attached to the TEM.

3. Results

Particle size of powders were decreased by ball milling process, even, nano-sized powders can be obtained by milling process. Activity of powders was increased because defect and broken bonds in powders were increased during ball milling. The solubility of carbon in metal is important for growth of nanotubes. We think that the solubility of carbon in iron may be increased by increasing activity of iron. So, the iron powders were milled by high energy ball mill.

XRD analyses of milled iron powders were shown in Fig. 1. XRD analysis shows that the crystal size is 17 nm. The narrow and high intensity peaks of samples show that the prepared powders are highly crystallized and the average crystallite size was calculated using a software TOPAZ 2 through the diffractions peaks from Scherer's formula [13] as shown below:

$$D = \frac{0.9\,\lambda}{\beta\, cos\theta}$$

where D is the crystal size, λ the X-ray wavelength, β the broadening of the diffraction peak and θ is the diffraction angle.

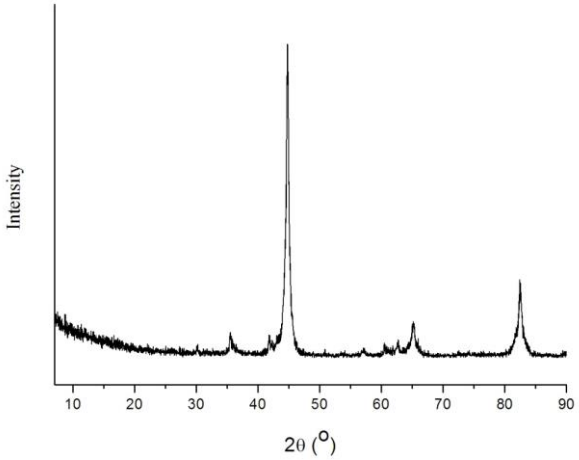

Fig. 1. XRD analysis of milled iron powder.

The crystallite size was also confirmed by using the transmission electron microscope (Fig. 2) which shows that Fe particles formed in agglomerated and separated nanosized structure. It is showed that nano-sized iron were successfully obtained by ball milling. In structure, the powders partly agglomerate because of particle size.

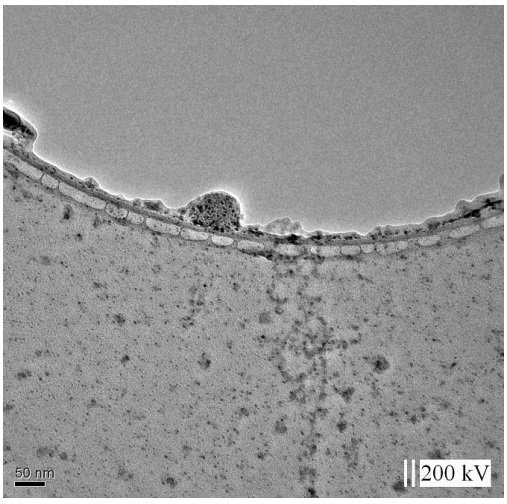

Fig. 2. HR-TEM image of milled iron powder.

In this study, carbon nanotubes were synthesized by chemical vapor deposition. In this process, the milled iron were used as catalyst to determinate the effect of milled iron on nanotubes growth. Fig. 3 shows the HR-TEM images of MWCNT synthesized in the flow reactor on activated iron particles. Products contain both thick nanotubes and thin nanotubes (Fig. 3.a and b). Thick nanotubes diameter are about 60 nm and thin nanotubes diameters are about 15 nm. HR-TEM characterization shows that these tubes consist of concentric parallel carbon sheets (Fig. 3c). The thin tubes consist of 10–12 carbon layers. The hollow core of these nanotubes is obvious. HR-TEM observations showed that some tubes were bent indicate that some defects (indicated by an arrow Fig. 3.b) occurred during the growth, leading to a change in the growth direction. It seems that during the growth process, pentagons or heptagons were inserted inside the hexagons network resulting to the topologic change of the tube [14]. HR-TEM studies reveal that the MWNTs were produced by the so-called tip growth mechanism, since the Fe catalyst nanoparticles are encapsulated on the nanotube closed tip (Fig. 3b and d). Some iron particles were observed inside the carbon nanotube bodies (arrow in Fig. 3b-d) which indicates that during the growth process some iron was carried out of the support surface by the tube growth and then remain encapsulated inside the tube channel. These encapsulated iron particles were no longer accessible by the reactants and resulting to the final complete deactivation of the catalyst for MWNT growth [15].

It is well known that catalyst particle size is a decisive parameter in growing CNTs and vapor-grown carbon fibers (VGCFs) [16]. In the catalytic chemical vapor deposition (CVD) method, the diameter of grown CNTs is almost equal to that of the catalyst particles [17,18]. Some authors [19] have also reported that an optimized catalyst particle size allows a good balance between the rates of hydrocarbon decomposition and carbon filament growth. Catalyst particles inside the nanotubes shown that nano-sized iron particles were successfully obtained by ball milling process.

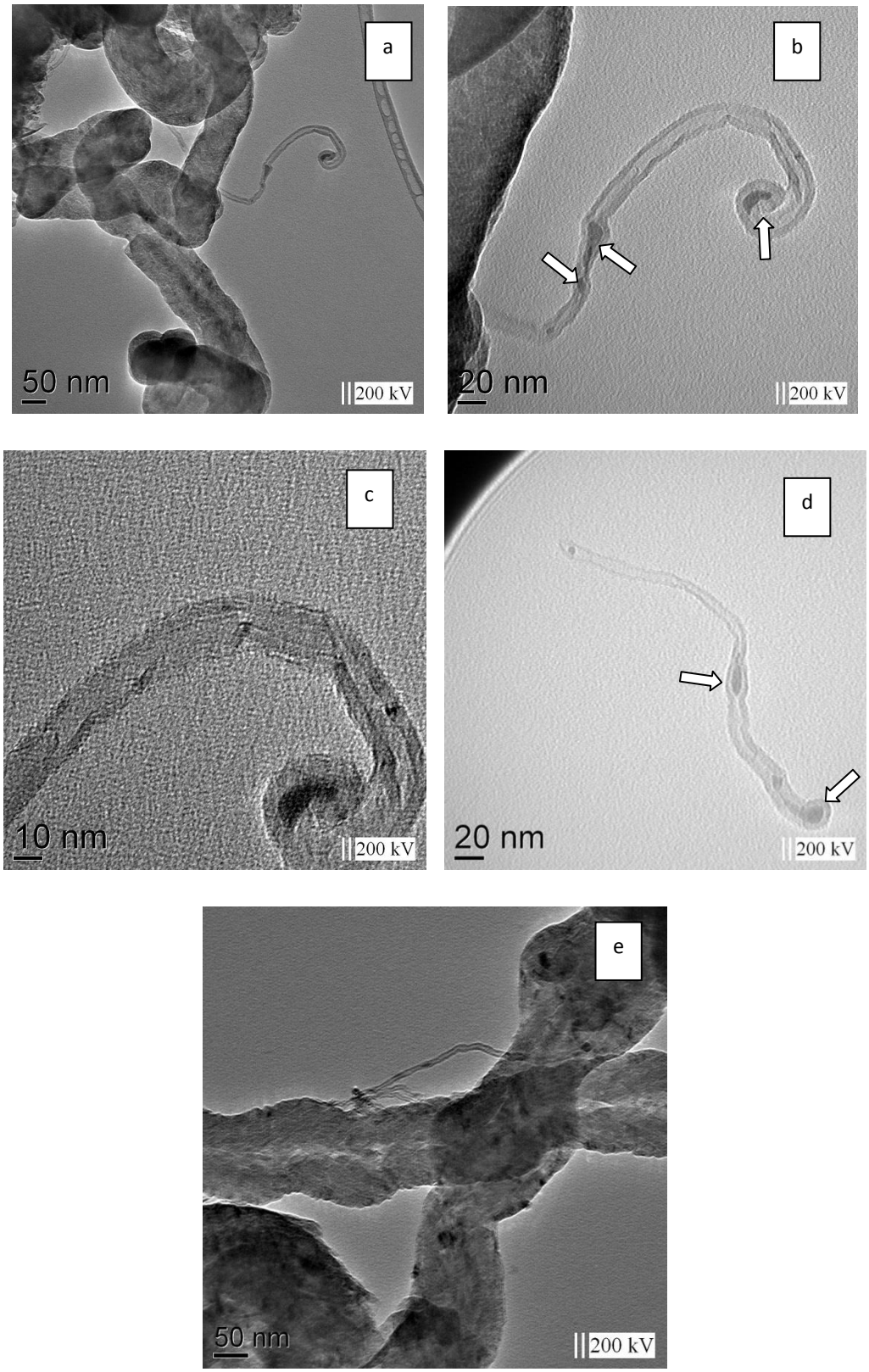

Fig. 3. HR-TEM images of carbon nanotubes produced by CVD.

The carbon filaments growth model generally adopted is based on the concepts of the VLS (vapor–liquid–solid) theory developed by Wagner and Ellis [21]. In this model, molecular decomposition and carbon solution are assumed

to occur at one side of the catalytic particle, which then becomes supersaturated [20,22]. Carbon diffuses from the side where it has been decomposed to another side where it is precipitated from solution [23]. It is not clear at this point of the model which is the driving force for carbon diffusion within the catalytic particle. For many authors, this force originates from the temperature gradient created in the particle by exothermic decomposition of the hydrocarbon at the exposed front faces and endothermic deposition of carbon at the rear faces, which are initially in contact with the support face [23,24]. Others ascribed the driving force to a concentration gradient [22,25]. However, because of a much lower surface energy of the basal planes of the graphite compared with the prismatic planes, it is energetically favorable for the filament to precipitate with the basal planes as the cylindrical planes [22]. The metal–support interactions are found to play a determinant role for the growth mechanism [22,26]. Weak interactions yield tip-growth mode whereas strong interactions lead to base-growth. Both growth modes are schematically shown in Fig. 4.

This growth model for carbon filaments has been widely used for carbon nanotubes. However, the specificity of the growth of nanotubes on nanoparticles with regard to the growth of carbon filaments is their nanometer dimensions. The energetic argument of the precipitation of carbon on its low-energy basal planes is for example no longer valid since the curving of the graphite layers introduces an extra elastic term into the free-energy equation of nucleation and growth, leading to a lower limit of about 10 nm [20,22]. Other mechanisms are therefore necessary to explain the growth of CNTs, whose diameter can be much smaller than this lower size limit [27]. In the catalytic growth of CNTs, not the ‘‘fluid nature’’ of the metal particle as in the VLS model has to be considered but the chemical interactions between the transition metal 3d electrons and the π carbon electrons [28]. Nanoparticles exhibit a very high surface energy per atom. The carbon in excess present during CVD process could solve this energetic problem by assembling a graphene cap on the particle surface with its edges strongly chemisorbed to the metal. Since the basal planes of graphite has an extremely low surface energy, the total surface energy diminishes. This is the Yarmulke mechanism proposed by Dai et al. [29]. The hemifullerene cap so formed on the partially carbon-coated particle lifts off and additional carbon atoms are continuously added to the edge of the cap, forming a hollow tube with constant diameter which grows away from the particle [30]. The driving force for the lifting process is believed to originate from the free energy release due to relaxation of the strain built up in the carbon cap around the spherical surface of the catalyst nanoparticle when carbon fragments assemble to form a CNT [31,32].

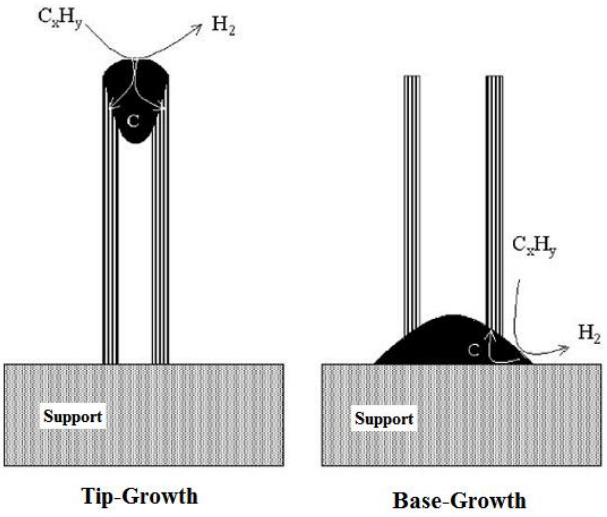

Fig. 4. The two growth modes of filamentous carbon [20].

The finite solubility for carbon of 3d-metals in certain temperature ranges [20,33] may play an important part in the growth process, since, once the hydrocarbon molecules are broken, carbon atoms are believed to diffuse into the catalyst particle, leading to supersaturation of carbon in the metal, as explained above. This process can eventually yield formation of carbides. For the role of solubility of carbon in the metal catalyst, Kock et al. e.g. claimed that high carbide contents are required before nucleation of carbon filaments proceeds [34]. Fe_3C has been detected during CNT growth process on iron nanoparticles and it was suggested that it may be the real catalyst [20,35,36]. In the VLS growth model, hydrocarbon dissociates to lead to formation of a metal carbide. This dissociation process requires a catalyst that is the metal. The next step of the growth process is carbon diffusion within the nanoparticle, followed by precipitation and CNT growth. If the driving force for carbon diffusion is a concentration gradient within the nanoparticle, the composition of the nanoparticle cannot be homogeneous, otherwise the catalyst would not be active anymore.

İn this study, thick nanotubes were formed as product and we think that surface of nanotubes were coated by carbon. A disorganized carbon coating at the surface of the nanotubes, which thickness increases with the acetylene concentration (with decreasing velocity), is observed in the TEM 002 lattice fringes images. Hence, the diameter change of MWNTs produced on Fe catalyst is related to the formation of an amorphous carbon coating on the nanotubes surface. The linear variation of the nanotube diameter with the gas flow velocity suggests that the residence time of acetylene in the reactor is controlling the amount of disorganized carbon coating and thus the tube diameter.

In addition, all of iron particle cannot be obtained the same size by ball milling process. So, milled powders contain higher sized particle and we think that the any thick nanotubes may grow on these coarse particles

Iron powders were milled by high energy ball milling in order to transform nano-sized iron particle. In addition, free energy of nano-sized iron particles were increased and transformation temperatures were decreased during milling process. In our experiments, γ-iron were formed at 650 ^{o}C although α-γ transformation were taken place at 727 ^{o}C. Supersaturating of carbon in nano-sized iron catalyst were exceedingly increased by ball milling process. We think that amorphous carbon coating at the surface of the nanotubes were increased because of the increasing carbon solubility of iron particles. Consequently, the acetylene concentration is more than enough for our experiments because of exceed increasing the carbon solubility of iron.

4. Conclusion

Iron particles sizes were decreased and the carbon solubility of iron were increased by milling process. Thin carbon nanotubes (about 15 nm) were obtained in experiments, but thick carbon nanotubes (about 60 nm) also formed. The surfaces of thick nanotubes were coated by amorphous carbon because of increasing the solubility of carbon in iron catalyst and acetylene concentration amount.

Our studies continue for decreasing of nanotubes diameters, optimization of iron catalyst and decreasing of amorphous carbon.

References

[1] S. Iijima, Nature **354**, 56 (1991).
[2] A. M. Fennimore, L. T. Cheng, D. H. Roach, Diamond Relat. Mater. **17**, 2005 (2008).
[3] A. Pasquini, G. B. Picotto, M. Pisani, Sens. Actuators A **123–124**, 655 (2005).
[4] M. Gong, T. Han, C. Cai, T. Lu, J. Du, J. Electrochem. **623**, 8 (2008).
[5] Ö. Güler, E. Evin, Optoelectron. Adv. Mater. – Rapid Comm. **6**, 183 (2012).
[6] Y. Maeda, Y. Takano, A. Sagara, M. Hashimoto, et. al., Carbon **46**, 1563 (2008).
[7] K. C. Mondal, A. M. Strydom, R. M. Erasmus, J. M. Keartland, N. J. Coville, Mater. Chem. Phys. **111**, 386 (2008).
[8] C. E. Baddour, F. Fadlallah, D. Nasuhoglu, R. Mitra, L. Vandsburger, J. Meunier, Carbon **47**, 313 (2008).
[9] Y. Tu, Z. P. Huang, D. Z. Wang, J. G. Wen, Z. F. Ren. Appl. Phys. Lett. **80**, 4018 (2002).
[10] H. J. Jeong, S. Y. Jeong, Y. M. Shin, J. H. Han, S. C. Lim, S. J. Eum, et al., Chem. Phys. Lett. **361**, 189 (2002).
[11] G. Bertoni, C. Cepek, F. Romanato, C. S. Casari, A. L. Bassi, C. E. Bottani, et al., Carbon **42**, 440 (2004).
[12] Z. P. Huang, D. L. Carnahan, J. Rybczynski, M. Giersig, M. Sennett, D. Z. Wang, et al. Appl. Phys. Lett. **82**, 460 (2003).
[13] X. He, Q. Z. Ling, Mater. Lett. **4284**, 1 (2002).
[14] G. Gulino, R. Vieria, J. Amadou, et.al., Appl. Catalysis A **279**, 89 (2005).
[15] R. T. K. Baker, P. S. Harris, The formation of filamentous carbon. In: Walker PL, Thrower PA, editors. Chemistry and Physics of Carbon. New York: Marcel Dekker, Inc.; 1978. p. 83–165.
[16] M. Yudasaka, R. Kikuchi, Y. Ohki, E. Ota, S. Yoshimura, Appl Phys Lett **70**, 1817 (1997).
[17] K. Hernadi, A. Fonseca, J. B. Nagy, D. Bernaerts, A. Lucas, Carbon **34**, 1249 (1996).
[18] A. K. M. Kibria, Y. H. Mo, K. S. Nahm, M. J. Kim, Carbon **40**, 1241 (2002).
[19] M. A. Ermakova, D. Y. Ermakov, L. M. Plyasova, G. G. Kuvshinov, Catal Lett, **62**, 93 (1999).
[20] A. C. Dupuis, Progress in Mat. Sci. **50**, 929 (2005).
[21] R. S. Wagner, W. C. Ellis, Trans AIME **233**, 1053 (1965).
[22] G. G. Tibbetts, J. Cryst. Growth. **66**, 632 (1984).
[23] R. T. K. Baker, Carbon **27**, 315 (1989).
[24] H. Kanzow, A. Ding, Phys. Rev. B **60**, 11180 (1999).
[25] J. R. Rostrup-Nielsen, D. L. Trimm, J. Catal. **48**, 155 (1977).
[26] A. M. Cassel, A. Raymakers, J. Kong, H. Dai, J. Phys. Chem. B **103**, 6484 (1999).
[27] P. M. Ajayan, T. W. Ebbesen, Rep. Prog. Phys. **60**, 1025 (1997).
[28] J-C. Charlier, S. Iijima, Growth mechanisms of carbon nanotubes, Topics. Appl. Phys. **80**, 55 (2001).
[29] H. Dai, A. G. Rinzler, P. Nikolaev, A. Thess, D. T. Colbert, R. E. Smalley, Chem. Phys. Lett. **260**, 471 (1996).
[30] P. Nikolaev, M. Bronikowski, R. Bradley, F. Rohmund, D. Colbert, K. Smith, et al., Chem. Phys. Lett. **313**, 91 (1999).
[31] V. Vinciguerra, F. Buonocore, G. Panzera, L. Occhipinti, Nanotechnology **14**, 655 (2003).
[32] R. Seidel, G. S. Duesberg, E. Unger, A. P. Graham, M. Liebau, F. Kreupl, J. Phys. Chem. B **108**, 1888 (2004).
[33] H. Dai, Surf. Sci. **500**, 218 (2002).
[34] A. Kock, P. K. De Bokx, E. Boellaard, W. Klop, J. W. Geus, J. Catal. **96**, 468 (1985).
[35] K. Nishimura, N. Okazaki, L. Pan, Y. Nakayama. Jpn J. Appl. Phys. **43**, 471 (2004).
[36] M. Cabero, I. Ramos, A. Ruiz, J. Catal. **215**, 305 (2003).

*Corresponding author: oguler@firat.edu.tr